Nonlinear pulse propagation in one-dimensional metal-dielectric multilayer stacks: Ultrawide bandwidth optical limiting

Michael Scalora,[1] Nadia Mattiucci,[2,3] Giuseppe D'Aguanno,[2] MariaCristina Larciprete,[4] and Mark J. Bloemer[1]
[1]*Charles M. Bowden Research Center, AMSRD-AMR-WS-ST, RDECOM, Redstone Arsenal, Alabama 35898-5000, USA*
[2]*Time Domain Corporation, Cummings Research Park, 7057 Old Madison Pike, Huntsville, Alabama 35806, USA*
[3]*Dipartimento di Fisica "E. Amaldi," Università "Roma Tre," Via Della Vasca Navale 84, I-00146 Rome, Italy*
[4]*INFM at Dipartimento di Energetica, Universita di Roma "La Sapienza," Via A. Scarpa 16, 00161 Roma, Italy*
(Received 26 September 2005; published 12 January 2006)

We numerically study the nonlinear optical properties of metal-dielectric photonic band gap structures in the pulsed regime. We exploit the high $\chi^{(3)}$ of copper metal to induce nonlinear effects such as broadband optical limiting, self-phase modulation, and unusual spectral narrowing of high intensity pulses. We show that in a single pass through a typical, chirped multilayer stack nonlinear transmittance and peak powers can be reduced by nearly two orders of magnitude compared to low light intensity levels across the entire visible range. Chirping dielectric layer thickness dramatically improves the linear transmittance through the stack and achieves large fields inside the copper to access the large nonlinearity. At the same time, the linear properties of the stack block most of the remaining electromagnetic spectrum.

DOI: 10.1103/PhysRevE.73.016603 PACS number(s): 42.70.Qs, 42.65.Pc, 42.65.Jx

I. INTRODUCTION

The subject of optical limiting and switching is important for optoelectronic applications. To date, most studies of optical limiting have focused on the ability of bulk materials to activate a complex, third order nonlinearity which thanks to the two-photon absorption component (imaginary nonlinear $\chi^{(3)}$) is capable of reducing longitudinal energy flow [1,2]. Metal nanoparticles may also be found interdispersed within a holding matrix [3,4], but in all cases the approach typically provides a nonlinear response over a relatively narrow wavelength range that does not exceed a few nanometers. The reason for this is that there is no known natural or artificial material that offers truly broadband shielding across the entire usable electromagnetic spectrum while remaining transparent in the visible range for ambient light intensities.

An alternative approach to optical limiting and switching of short pulses was introduced within the context of all-dielectric photonic band gap (PBG) structures and a third order nonlinearity [5,6], albeit still within the confines of narrow-band operation. The concept utilized field localization effects near the photonic band edge, where the field intensity is generally enhanced in a manner that is roughly proportional to the density of modes [7]. This may be several orders of magnitude larger compared to ordinary bulk materials, depending on the geometry of the multilayer stack. As the field tunnels through the stack, at high intensities it dynamically changes the local index of refraction, which alters the local band structure, effectively tuning the carrier frequency of the pulse inside the gap region [5,6].

Band edge optical limiting of the kind predicted in Ref. [5] was later experimentally demonstrated in two different contexts: (i) in an all-dielectric (AD) PBG composed of ZnSe and MgF_2 layers [8]; and (ii) in a one-dimensional metal-dielectric (MD) PBG [9,10] composed of Ag and ZnO layers [11]. In Ref. [8], a shift of the band edge was observed as a change of the optical path of ZnSe occurred under intense field illumination and heating. In Ref. [11], the two-photon absorption of ZnO and field localization effects were uniquely exploited to experimentally reduce the nonlinear transmittance in the visible range (532 nm incident wavelength) by almost a factor of 2 compared to linear transmission.

The propagation of light inside metals has not generally been the subject of any focused investigation because, as is well-known, metals are highly reflective at almost any incident wavelength. Based on the Drude model, the relative transparency threshold generally depends on the plasma frequency, found at approximately 580 nm for Cu, 320 nm for Ag, and 200 nm for Al [12]. However, the metal-dielectric photonic band gap (MDPBG) introduced in Refs. [9,10] changed all that and demonstrated that it was possible to render metals transparent not necessarily near regions where one expects them to be transparent, i.e., near their plasma resonance [13], but also well into the Drude region, where conventional wisdom holds that metals are opaque. In fact, the photonic band gap approach allows even hundreds of nanometers of layered MDPBG to become transparent in the $3-5$ μm range [9,10] and beyond, provided appropriate metals, thicknesses, and dielectric materials are chosen. This is due to the fact that geometrical dispersion (layering) adds to material dispersion to modify the effective overall dispersive response of a given composite structure [14]. Thus, from a practical point of view, in addition to opening new avenues of research, the ability to use metals for both linear and nonlinear optical applications that require relatively high transmission and sharp cutoffs is of some technological importance [9–11].

More recently it was pointed out that transparent metal stacks made with Cu and SiO_2 layers could be used to access the nonlinearity of the metal itself [15,16]. This is due to the fact that as the field tunnels through the stack a good fraction of the energy can still be found inside the metal layers, the magnitude of skin depth notwithstanding [9]. Because the

third order nonlinear coefficients of metals may be several orders of magnitude larger than that of ordinary semiconductors (Cu $\sim 10^{-6}$ esu and Ag $\sim 10^{-8}$ esu) [3,4], nonlinear effects may be enhanced beyond what is possible to achieve for ordinary materials. In addition to enhanced phase modulation effects [15], the nonlinear transmittance could also be modified by the action of two-photon absorption inside the metal layers [16]. But regardless of the physical origin of the $\chi^{(3)}$, once the field engages it under pulsed conditions, a changing nonlinear transmittance (or reflectance) is indicative of a combination of a dynamically shifting photonic band edge and changing effective absorption [5,11,16]. Given the generic neglect of propagation effects inside metals, we are thus motivated to develop an easily implementable and physically transparent model to study linear and nonlinear pulse propagation inside MDPBG stacks similar to those found in the cited literature.

II. TRANSPARENT METALS

We begin by asking the following questions: what linear transmittance is possible to achieve given a certain total metal thickness, and what is then the best way to access metal nonlinearities within a given wavelength range? The structure investigated in Ref. [15,16] was designed primarily to maximize field amplitude inside the metal layers to take advantage of the nonlinearity, but at the expense of linear transmittance. The result is a nonresonant structure, with dielectric layers roughly $\lambda/4$ in thickness instead of the multiple of $\lambda/2$ needed for resonance tunneling and higher transmission values [9–11]. Indeed, the passband of Ref. [16] appears to be just a perturbation of the transparency that naturally occurs near the plasma frequency of Cu, at $\sim$580 nm. In reality it is not necessary to sacrifice transmission at the expense of field localization inside the metal layers. For example, one could use a high index material, such as ZnO or TiO_2, instead of SiO_2. One may also resort to chirping layer thickness, which accomplishes at least three things: (i) it can nearly double linear transmittance; (ii) it can significantly improve visibility through the stack by flattening and smoothing the transmission band and by reducing unwanted reflections within the passband to a minimum; and (iii) it improves field localization inside the metal layers. In short, while in the resonant structure the metal layers act more like mirrors, chirping the layers makes the structure nonresonant, and the light propagates with less opposition.

In Fig. 1 we show the linear transmittance of three different structures: (i) that of Ref. [16], which exhibits a maximum transmission around 20% at 650 nm; (ii) a structure with the same geometry as in (i) above, but with SiO_2 layer thickness approximately $\lambda/2$; and (iii) an MDPBG stack that contains the same number and thickness of Cu layers, but that uses high index ($n \sim 2$) ZnO, with entrance and exit layers half as thick as the inner layers (chirping). The figure shows that the combination of the high index material and chirping leads to transmittance levels of approximately 70% in the neighborhood of 650 nm, with average transmittance well above 50% throughout the entire passband. At the same time, field values inside the chirped structure can be several

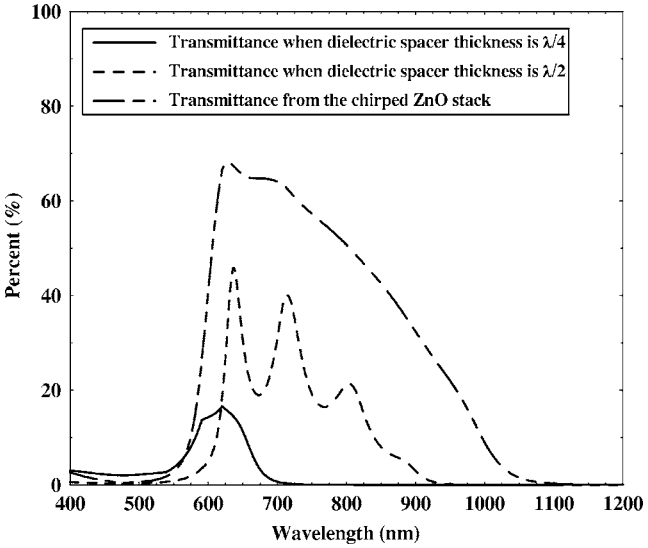

FIG. 1. Transmittance function for three different stacks. Each structure has 5, 16 nm Cu layers, while dielectric spacer thickness varies from 96 nm (solid curve) to approximately 200 nm (short dashes). The highest transmittance is obtained (short and long dashes) by using a high index material, and by halving the thickness of the entrance and exit ZnO layers.

times larger than field values found in the periodic, resonant stack [9–11], and of the same order as incident field values [15,16]. While the transmittance from the chirped stack at 650 nm is approximately 140 times larger than the transmittance from a single, 80 nm, uniform Cu layer, further optimizations are possible by refining material choices, thicknesses, and number of layers.

The linear transmittance that is possible to achieve by layering metals is thus truly extraordinary, with a passband that may be several hundreds of nanometers wide, and encompasses the entire visible range, for example. At the same time, the rest of the usable electromagnetic spectrum is rejected: at longer wavelengths any uniform amount of metal one can deposit is truly impregnable even to microwave fields [9]. At the opposite end of the spectrum, uv light can be removed by either interband transitions in the case of Cu [16], or by designing an interferometric gap to coincide with the uv region, if other metals such as Ag [9–11] or Al are used. Thus a number of geometrical factors may be combined to yield highly transparent, conductive MDPBG stacks, while relatively high field values can still be achieved within the metal layers.

As a further consideration, it is generally desirable to access the particularly high nonlinearity of Cu within the entire visible range. Indeed if the nonlinear properties of Cu could be effectively accessed while retaining high linear transmittance, one would then be in a position to accomplish what is currently deemed impossible, namely to obtain an ultrawide band optical limiter that utilizes the linear and nonlinear optical properties of Cu metal to affect and control the transmission of light over the entire usable electromagnetic spectrum, with a remarkably simple structure only a few hundred nanometers thick.

In Fig. 2 we plot transmittance and reflectance of a device potentially capable of accomplishing precisely this. It con-

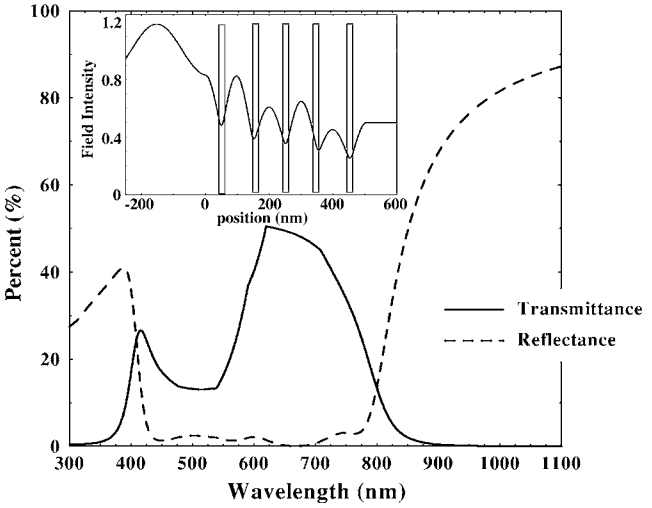

FIG. 2. Linear transmittance and reflectance from a chirped, 5 1/2periods of a layered Cu(15 nm)/ZnO(86 nm) stack. The first and last ZnO layers are 43 nm thick.

sists of a chirped Cu (five layers, each 15 nm thick)/ZnO ($n \sim 2$) stack, where internal ZnO layers are 86 nm thick, and external layers are approximately 43 nm thick, to maximize transmittance. The choice of ZnO is by no means unique, and in fact one may use almost any other dielectric or semiconductor material that will adhere to the contiguous metal. However, the two-photon absorption coefficient of ZnO, which is reported to be $\beta \sim 2$ cm/GW in the visible range, under certain conditions has been measured to be as high as 500 cm/GW in the 700 nm region [17]. This may be extremely useful if a device is to operate in that range. The inset of Fig. 2 shows the field intensity distribution inside the grating for an incident wavelength of approximately 632 nm. The peculiarity of this kind of structure is that similar field localization (of the same order as the input field) occurs within the entire transparency region (400–800 nm), suggesting that nonlinear effects may be excited at any wavelength inside that range with almost the same efficacy, depending on the dispersion and magnitude of the nonlinear coefficient.

III. PULSE PROPAGATION MODEL

Although the formalism of our propagation model is developed in detail elsewhere [18,19], it is worthwhile to provide here the most salient points. We assume that the dispersion function can be written as a general Taylor expansion/series:

$$\begin{aligned}\varepsilon(\mathbf{r},\omega) = & \ \varepsilon(\mathbf{r},\omega_0) + \left.\frac{\partial \varepsilon(\mathbf{r},\omega)}{\partial \omega}\right|_{\omega_0} (\omega-\omega_0) \\ & + \ \frac{1}{2}\left.\frac{\partial^2 \varepsilon(\mathbf{r},\omega)}{\partial \omega^2}\right|_{\omega_0} (\omega-\omega_0)^2 + \cdots \\ & = a(\mathbf{r},\omega_0) + b(\mathbf{r},\omega_0)\omega + c(\mathbf{r},\omega_0)\omega^2 + \cdots . \end{aligned} \quad (1)$$

The spatial dependence is meant to include spatial discontinuities, as in our case, or other types of spatial inhomogeneities. The field is assumed to be linearly polarized, and is separated into a generic envelope function, not necessarily slowly varying, and a carrier frequency, as follows: $E_x(\mathbf{r},t) = E(\mathbf{r},t)e^{-i\omega_0 t}$. Then, given the following constitutive relation between the displacement vector to the electric field:

$$\begin{aligned} D_x(\mathbf{r},t) &= \int_{-\infty}^{\infty} \varepsilon(\mathbf{r},\omega)E_x(\mathbf{r},\omega)e^{-i\omega t}d\omega \\ &= \int_{-\infty}^{\infty} \{a(\mathbf{r},\omega_0) + b(\mathbf{r},\omega_0)\omega + c(\mathbf{r},\omega_0)\omega^2 + \cdots\} \\ &\quad \times [E_x(\mathbf{r},\omega)]e^{-i\omega t}d\omega \end{aligned} \quad (2)$$

it is easy to show that [18–20]:

$$\begin{aligned}\frac{\partial D_x(\mathbf{r},t)}{\partial t} = \Bigg\{ & -i\omega_0\varepsilon(\omega_0)E + \left[\frac{\partial[\omega\varepsilon(\omega)]}{\partial\omega}\right]_{\omega_0}\frac{\partial E}{\partial t} \\ & + \frac{i}{2}\left[\frac{\partial^2[\omega\varepsilon(\omega)]}{\partial\omega^2}\right]_{\omega_0}\frac{\partial^2 E}{\partial t^2} + \cdots \Bigg\} e^{-i\omega_0 t}, \end{aligned} \quad (3)$$

which in turn can be expressed in a more compact form as [19]

$$\frac{\partial D_x(\mathbf{r},t)}{\partial t} = -\sum_{n=0}^{\infty}\left\{ i^{n+1} \left.\frac{\partial^n(\omega\varepsilon)}{\partial\omega^n}\right|_{\omega=\omega_0} \frac{1}{n!}\frac{\partial^n E}{\partial t^n}\right\} e^{-i\omega_0 t}. \quad (4)$$

Equation (4) can then be used to write Maxwell's equations, which with one longitudinal dimension and time can be written as follows [18,19]:

$$\begin{aligned} & \alpha\frac{\partial E}{\partial\tau} + i\frac{\alpha'}{4\pi}\frac{\partial^2 E}{\partial\tau^2} - \frac{\alpha''}{24\pi^2}\frac{\partial^3 E}{\partial\tau^3} + \cdots \\ & \quad = i\beta[(\varepsilon(\xi) + 6\chi^{(3)}|E|^2)E - H] - \frac{\partial H}{\partial\xi} - 12\pi\chi^{(3)}\frac{\partial(|E|^2 E)}{\partial\tau}, \\ & \frac{\partial H}{\partial\tau} = i\beta(H-E) - \frac{\partial E}{\partial\xi}. \end{aligned} \quad (5)$$

Here $\alpha = \partial[\tilde{\omega}\varepsilon(\xi)]/\partial\tilde{\omega}$ is a parameter directly related to the group velocity of the pulse [18], $\alpha' = \partial^2[\tilde{\omega}\varepsilon(\xi)]/\partial\tilde{\omega}^2$, and so on, $\beta = 2\pi\tilde{\omega}$. We have explicitly expanded the summation of Eq. (4) and show only four terms of that infinite series, three on the left-hand side and the linear term on the right-hand side. The following scaling has been adopted: $\xi = z/\lambda_r$, $\tau = ct/\lambda_r$, and $\tilde{\omega} = \omega/\omega_r$, where $\lambda_r = 1$ μm is conveniently chosen as the reference wavelength. Equations (5) contain no approximations, but given the nature of the typical MDPBG stack, they can be simplified byneglecting second and higher order, material dispersion terms, i.e. $\alpha(\partial E/\partial\tau) \gg i(\alpha'/4\pi)\partial^2 E/\partial\tau^2$. This condition can be satisfied rather easily in at least four ways with: (i) a relatively slowly varying dispersion function; (ii) a relatively slowly varying field envelope function; (iii) a combination of (i) and (ii); and (iv) a relatively short distance of propagation. It is worth considering a typical case that exemplifies all cases under consideration, to clarify the nature of this approximation/condition.

First, the dispersion functions of typical metals vary relatively slowly over ranges that may span hundreds of nanometers. For example, within the 630–800 nm range, the real part of the material dispersion of Cu can be reproduced quite well from the following expression: $\mathrm{Re}[\varepsilon(\tilde{\omega})\tilde{\omega}]=-11.6\tilde{\omega}^2+70.6\tilde{\omega}-102$, which yields an approximately linear dielectric function with slight curvature. It is then easy to verify that within the specified range the ratio between the first and second order coefficients is $|\alpha|/(|\alpha'|/4\pi)\sim 20$. Second, typical lengths of finite PBG structures are just a few tens of microns [14], far shorter than typical dispersion lengths of any bulk material. In the case of MDPBGs, a typical stack may be less than 500 nm thick, with less than 100 nm of total metal. This means that higher order dispersion effects remain much smaller then the geometrical dispersion arising from spatial, material discontinuities [14]. Third, we use pulses that, although short, may be several tens of wave cycles in duration, to insure that the nonlinear response it always faster than pulse duration to take full advantage of it. Taking these factors together, and assuming the envelope's period (pulse width) is τ_p wave cycles, it generally means that $|\alpha\dot{E}|/(|\alpha'\ddot{E}|/4\pi)\sim 20\tau_p$. Our calculations in fact show that, on average, $|\alpha\dot{E}|/(|\alpha'\ddot{E}|/4\pi)\sim 100$ for a 5-optical cycle pulse, and $|\alpha\dot{E}|/(|\alpha'\ddot{E}|/4\pi)\sim 40$ for a 2-optical cycle pulse during the entire interaction. Therefore, neglect of higher order dispersion terms is completely justified even for pulses just a few wave cycles in duration. Thus if we assume that the expansion in Eq. (4) can be rewritten by retaining only the first two leading terms, the equations then simplify to [18,19]

$$\alpha\frac{\partial E}{\partial\tau}=i\beta[(\boldsymbol{\varepsilon}(\chi)+6\boldsymbol{\chi}^{(3)}|E|^2)E-H]-\frac{\partial H}{\partial\xi}-12\pi\chi^{(3)}\frac{\partial(|E|^2E)}{\partial\tau},$$

$$\frac{\partial H}{\partial\tau}=i\beta(H-E)-\frac{\partial E}{\partial\xi}. \tag{6}$$

Integration of Eqs. (6) is carried out using a fast Fourier transform-based algorithm [21] capable of handling all orders of feedback. We use a spectral method primarily because it involves multiplication of linear operators; it is unconditionally stable, with no known issues relating to phase or amplitude errors, and thus not prone to the generation of any numerical artifacts; and it can easily be extended to the multidimensional domain almost effortlessly [18].

IV. RESULTS AND DISCUSSION

We analyze pulse propagation in the MDPBG stack of Fig. 2. In Fig. 3 we show a plot of both linear and nonlinear transmittance across the visible and near IR portion of the spectrum. Although some dispersion of the nonlinear coefficient is to be expected [16] and can easily be taken into account, for simplicity we assume $\chi^{(3)}_{\mathrm{Cu}}\sim(10^{-9}+i10^{-6})$ esu [3,4,15,16], and $\chi^{(3)}_{\mathrm{ZnO}}\sim(10^{-12}+i10^{-10})$ esu [17], at all wavelengths investigated. However, because in this case the nonlinear coefficient of Cu is so much larger than that of ZnO, the inclusion of the nonlinearity in the ZnO layers matters very little. Figure 3 was generated using incident pulses that are approximately 1 ps in duration to ensure nearly instantaneous nonlinear response, with peak field intensities of approximately 15 GW/cm^2. The figure suggests that while linear MDPBGs can block most of the spectrum by opening a single transparency window in the visible range, this entire window can be dynamically closed through a nonlinear optical limiting process that accesses the very large nonlinearity of copper. Overall transmission and peak powers decrease by almost two orders of magnitude across the entire visible range with a single pass through the stack.

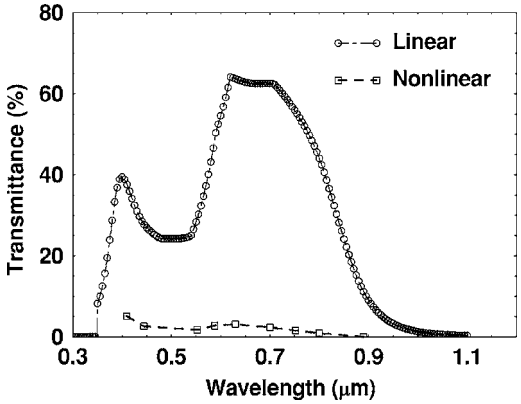

FIG. 3. Linear and nonlinear transmittance from the stack of Fig. 2. Each nonlinear data point was obtained by propagating a Gaussian pulse approximately 1 ps in duration, with a peak intensity of roughly 15 GW/cm^2.

In Fig. 4 we show typical incident, transmitted, and reflected pulses. We note that for a reference wavelength of 1 μm, the spatial extension of the pulse is approximately 150–200 μm, to be contrasted with a structure thickness of approximately 1/2 μm. We also remark that the spatial

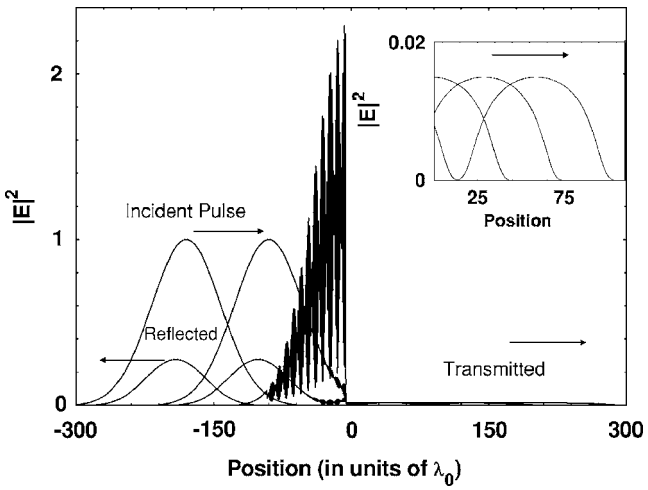

FIG. 4. Typical incident, transmitted, and reflected pulses from the structure of Fig. 2. The spatial width and temporal duration of the transmitted pulse increase, causing spectral narrowing. Inset: transmitted pulse.

width of the transmitted pulse increases by approximately 50% (inset), which corresponds to an increased temporal duration and to an unusually narrower spectral bandwidth. Although this behavior is unusual, indeed opposite to what one might expect based on ordinary self-phase modulation, which broadens the spectrum, it is possible to narrow the bandwidth of a pulse under the action of self-phase modulation (usually intended to mean an effect due to the real part of the nonlinear coefficient, $\mathrm{Re}[\chi^{(3)}]$), provided the incident pulse is prechirped appropriately [22,23]. However, we do not prechirp the pulse, and in all cases investigated $\mathrm{Im}[\chi^{(3)}] \gg \mathrm{Re}[\chi^{(3)}]$ for both Cu and ZnO. Neglecting the time derivative of the nonlinearity, the effect is then entirely due to two-photon absorption, which contributes to both the real and imaginary parts of the complex, instantaneous index of refraction via the relationship $n_{\mathrm{eff}}=n_r+in_i=(\varepsilon_{\mathrm{L}}+6\chi^{(3)}|E|^2)^{1/2}$, where ε_{L} is the linear dielectric function. The instantaneous index affects the local band structure [5,6], causes reversible band shifts, and changes the local absorption coefficient. We note that a complex $\chi^{(3)}$ does *not* contribute to the index of refraction in a symmetric fashion. All things being equal, exchanging the values of the real and imaginary parts of $\chi^{(3)}$ does not yield the same dynamic index, and can lead to spectral broadening. For example, if we assume that $\chi^{(3)}_{\mathrm{Cu}} \sim (10^{-6}+i10^{-9})$ esu, instead of $\chi^{(3)}_{\mathrm{Cu}} \sim (10^{-9}+i10^{-6})$ esu, then spectral narrowing is replaced by normal spectral broadening. In any case, the pulse tunnels through the stack and in fact acquires a very small chirp, as the structure is quite short. However, this shortcoming is compensated by the huge nonlinear coefficient, and thus spectral narrowing can occur.

In Ref. [15] it was predicted that the effective nonlinear coefficient for the entire MDPBG stack was of order $n_2 \sim 10^{-9}$ cm^2/W. The implication here is that with light intensities of order 1 GW/cm^2, the nonlinear index change can be of order unity, or several orders of magnitudes larger than is currently possible in ordinary semiconductors (δn $\sim 10^{-3}$–10^{-4}). Experimental results in [16] then suggested a change of $\mathrm{Im}(\delta\varepsilon) \sim 1$ occurs under illumination by a 25 ps, 200 MW/cm^2 pulse. Using 1 ps incident pulses of the same peak intensity, in Fig. 5 we show the instantaneous index of refraction: the real part of the index changes by approximately a factor of 2, from a minimum of 0.23 to approximately 0.4 (thin, solid curve). The imaginary part remains almost constant (thin, dashed curve). Reconstruction of the dielectric function then yields an $\mathrm{Im}(\delta\varepsilon)$ of order unity, just as the experiment suggests [16]. Similar dynamics occurs for incident pulses with peak intensities of 4 GW/cm^2, except that now $\mathrm{Im}(\delta\varepsilon) \sim 4$, and the real part of the index changes by a factor of 3, from 0.23 to approximately 0.65 (thick, solid curve), and some change in the imaginary part is now discernable (thin, dashed curve).

Finally, we fix the carrier frequency of the pulse at approximately 632 nm, and vary the peak intensity of the pulse. The result is Fig. 6, where we show nonlinear transmittance and reflectance, and total remaining energy as a function of input peak intensity. As nonlinear transmittance decreases monotonically, reflections increase. Increasing reflections are a clear sign that the effective local index of refraction changes [5,6], and that the local band edge shifts. Of course, we have not included dynamics that ensues from possible material breakdown, which may thwart our predictions for intensities well above 1 GW/cm^2. We note that for Au, similar in many ways to Cu, plasma formation is reported at 120 GW/cm^2 for incident, 290-fs pulses [24], and approximately 10 GW/cm^2 for 35 ps pulses [25]. Therefore we expect our structure to be able to withstand several tens of GW/cm^2, provided pulses are just a few picoseconds in duration.

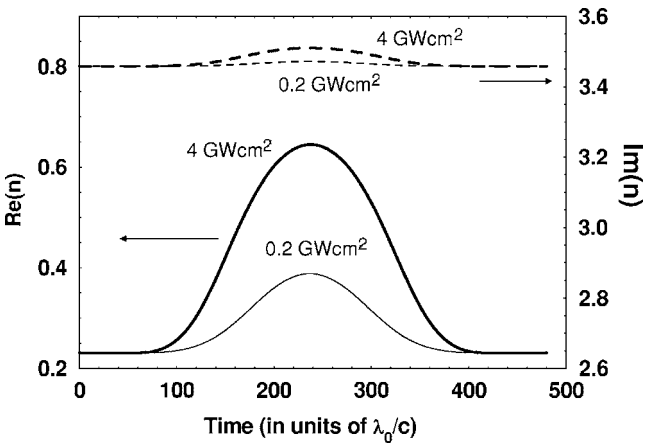

FIG. 5. Real (left axis, solid curves) and imaginary (right axis, dashed curves) parts of the effective index of refraction corresponding to the case of Fig. 4. Two cases are shown, for input intensities of 200 MW/cm^2 and 4 GW/cm^2.

V. CONCLUSIONS

We have conducted a numerical study of nonlinear pulse propagation phenomena in a multilayer, Cu/ZnO metal-dielectric photonic band gap structure, and find that the non-

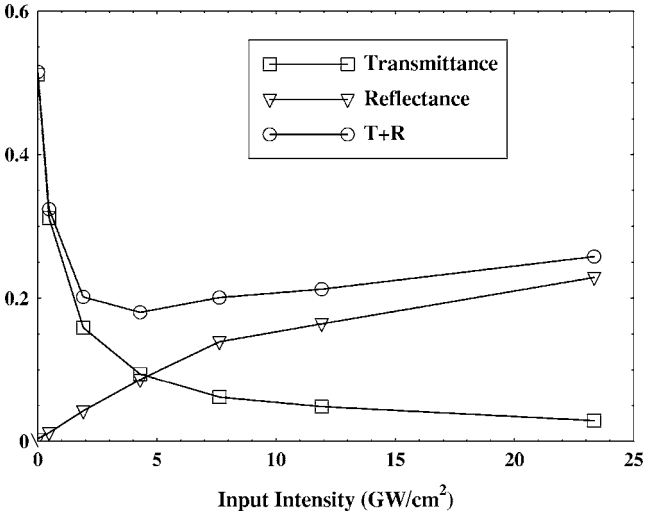

FIG. 6. Transmittance, reflectance, and total energy remaining (R+T) as a function of time. While increased two-photon absorption may help to explain a simple reduction of the transmitted energy, an increased reflection indicates that a dynamics shift of the band edge also occurs.

linearity of Cu may be exploited to yield ultrawide band optical limiting across the entire visible range. At high intensities, the transmittance can be reduced by nearly two orders of magnitude in a single pass through the stack, compared to ambient light levels. The remaining portion of the usable spectrum is rejected thanks to the linear properties of the stack. At the same time, the bandwidth of the transmitted pulse can be narrowed as a result of a combination of a dynamic chirp and high nonlinear coefficient. The location of the passband can be widely tuned, from visible wavelengths well into the near and mid-IR ranges, and within this range nonlinear effects explored in almost any region of interest. We expect that this type of device will have important applications for optical limiting purposes.

[1] E. W. Van Stryland, H. Vanherzeele, M. A. Woodall, M. J. Soileau, A. L. Smirl, S. Guha, and T. F. Boggess, Jr., Opt. Eng. **24**, 613 (1985); G. S. He, J. D. Bhawalkar, C. F. Zhao, and P. N. Prasad, Appl. Phys. Lett. **67**, 2433 (1995); M. Sheik-Bahae, D. C. Hutchings, D. J. Hagan, and E. W. Van Stryland, IEEE J. Quantum Electron. **27**, 1296 (1991); E. W. Van Stryland, M. A. Woodall, H. Vanherzeele, and M. J. Soileau, Opt. Lett. **10**, 490 (1985); S. Guha, E. W. Van Stryland, and M. J. Soileau, *ibid.* **10**, 285 (1985); Q. Li, C. Liu, Z. Liu, and Q. Gong, Opt. Express **13**, 1833 (2005).

[2] R. H. Stolen, J. P. Gordon, W. J. Tomlinson, and H. A. Haus, J. Opt. Soc. Am. B **6**, 1159 (1989).

[3] J. Olivares, J. Requejo-Isidro, R. del Coso, R. de Nalda, J. Solis, C. N. Afonso, A. L. Stepanov, D. Hole, P. D. Townsend, and A. Naudon, J. Appl. Phys. **90**, 1064 (2001); J. M. Ballesteros, R. Serna, J. Soli's, C. N. Afonso, A. K. Petford-Long, D. H. Osborne, and R. F. Haglund, Appl. Phys. Lett. **71**, 2445 (1997); R. del Coso, J. Requejo-Isidro, J. Solis, J. Gonzalo, and C. N. Afonso, J. Appl. Phys. **95**, 2755 (2004); Li Yang, K. Becker, F. M. Smith, R. H. Magruder III, R. F. Haglund, Jr., Lina Yang, R. Dorsinville, and R. R. Alfano, J. Opt. Soc. Am. B **11**, 457 (1994).

[4] K. Uchida, S. Kaneko, S. Omi, C. Hata, H. Tanji, Y. Asahara, A. J. Ikushima, T. Tokizaki, and A. Nakamura, J. Opt. Soc. Am. B **11**, 1236 (1994); Y. Hamanaka, A. Nakamura, N. Hayashi, and S. Omi, *ibid.* **20**, 1227 (2003); E. Mishina, K. Nagai, D. Barskyb, and S. Nakabayashi, Phys. Chem. Chem. Phys. **4**, 127 (2002).

[5] M. Scalora, J. P. Dowling, C. M. Bowden, and M. J. Bloemer, Phys. Rev. Lett. **73**, 1368 (1994).

[6] M. Scalora, J. P. Dowling, C. M. Bowden, and M. J. Bloemer, J. Appl. Phys. **76**, 20023 (1994).

[7] J. M. Bendickson, J. P. Dowling, and M. Scalora, Phys. Rev. E **53**, 4107 (1996); G. D'Aguanno, N. Mattiucci, M. Scalora, M. J. Bloemer, and A. M. Zheltikov, *ibid.* **70**, 016612 (2004); G. D'Aguanno, N. Mattiucci, M. Centini, M. Scalora, and M. J. Bloemer, *ibid.* **69**, 057601 (2004).

[8] M. C. Larciprete, C. Sibilia, S. Paoloni, G. Leahu, R. Li Voti, M. Bertolotti, M. Scalora, and K. Panajotov, J. Appl. Phys. **92**, 2251 (2002); M. C. Larciprete, N. Savalli, T. Tenev, M. Scalora, G. Leahu, C. Sibilia, S. Baglio, K. Panajotov, and M. Bertolotti, Appl. Phys. B: Lasers Opt. **81**, 245 (2005).

[9] M. Scalora, M. J. Bloemer, A. S. Manka, S. D. Pethel, J. P. Dowling, and C. M. Bowden, J. Appl. Phys. **83**, 2377 (1998); M. J. Bloemer and M. Scalora, Appl. Phys. Lett. **72**, 1676 (1998).

[10] M. Scalora, M. J. Bloemer, and C. M. Bowden, Opt. Photonics News **10**, 23 (1999).

[11] M. C. Larciprete, C. Sibilia, S. Paoloni, M. Bertolotti, F. Sarto, and M. Scalora, J. Appl. Phys. **93**, 5013 (2003).

[12] *Handbook of Optical Constants of Solids*, edited by E. D. Palik (Academic Press, New York, 1985).

[13] T. W. Ebbesen, H. J. Lezec, H. F. Ghaemi, T. Thio, and P. A. Wolff, Nature (London) **391**, 667 (1998).

[14] M. Centini, C. Sibilia, M. Scalora, G. D'Aguanno, M. Bertolotti, M. J. Bloemer, C. M. Bowden, and I. Nefedov, Phys. Rev. E **60**, 4891 (1999); M. Centini, M. J. Bloemer, K. Myneni, M. Scalora, C. Sibilia, M. Bertolotti, and G. D'Aguanno, Phys. Rev. E **68**, 016602 (2003); G. D'Aguanno, M. Centini, M. J. Bloemer, K. Myneni, M. Scalora, C. M. Bowden, C. Sibilia, and M. Bertolotti, Opt. Lett. **27**, 176 (2002); M. J. Bloemer, K. Myneni, M. Centini, M. Scalora, and G. D'Aguanno, Phys. Rev. E **65**, 056615 (2002).

[15] R. S. Bennink, Y. K. Yoon, R. W. Boyd, and J. E. Sipe, Opt. Lett. **24**, 1416 (1999).

[16] N. N. Lepeshkin, A. Schweinsberg, G. Piredda, R. S. Bennink, and R. W. Boyd, Phys. Rev. Lett. **93**, 123902 (2004).

[17] J. H. Lin, Y. J. Chen, H. Y. Lin, and W. F. Hsieha, J. Appl. Phys. **97**, 033526 (2005).

[18] M. Scalora, G. D'Aguanno, N. Mattiucci, M. J. Bloemer, J. W. Haus, and A. M. Zheltikov, Appl. Phys. B: Lasers Opt. **81**, 393 (2005).

[19] M. Scalora, M. Syrchin, N. Akozbek, E. Y. Poliakov, G. D'Aguanno, N. Mattiucci, M. J. Bloemer, and A. M. Zheltikov, Phys. Rev. Lett. **95**, 013902 (2005).

[20] L. D. Landau and E. M. Lifshitz, *Electrodynamics of Continuous Media* (Pergamon, New York, 1960), pp. 253–256.

[21] M. Scalora and M. E. Crenshaw, Opt. Commun. **108**, 191 (1994).

[22] S. A. Planas, N. L. Pires Mansur, C. H. Brito Cruz, and H. L. Fragnito, Opt. Lett. **18**, 699 (1993).

[23] E. R. Andresen, J. Thøgersen, and S. R. Keiding, Opt. Lett. **30**, 2025 (2005).

[24] N. A. Papadogiannis, P. A. Loukakos, and S. D. Moustaizis, Opt. Commun. **166**, 133 (1999).

[25] A. T. Georges and N. E. Karatzas, Appl. Phys. B: Lasers Opt. **81**, 479 (2005).